Available online at www.sciencedirect.com
ScienceDirect
Journal of Sound and Vibration 298 (2006) 877–891
JOURNAL OF SOUND AND VIBRATION
www.elsevier.com/locate/jsvi

Reconstruction of the interior sound pressure of a room using the probabilistic approach

Y.Y. Lee*, A.Y.T. Leung, H.F. Lam, H.Y. Sun

Department of Building and Construction, City University of Hong Kong, Kowloon Tong, Kowloon, Hong Kong, China

Received 10 March 2005; received in revised form 17 May 2006; accepted 29 May 2006
Available online 2 August 2006

Abstract

In this paper, a probabilistic approach is introduced and used to find the optimal values assigned to the uncertain parameters of a room acoustic model, which is used for the reconstruction of the interior sound pressure distribution. The acoustic model selected here to examine the capacity of the probabilistic approach is a rectangular room with two air leakages that is subject to an external uniform noise. The model is set up using the modal analysis method. The values of the uncertain parameters of the model are identified using the time domain sound pressure responses at selected measurement points. In the simulation results, the comparisons between the proposed approach and the typical least error square method show that the former clearly assigns optimal values to the uncertain model parameters for the best prediction, while the latter generates a set of values for which the prediction errors are very similar and close to the minimum (in other words, it is difficult to identify the optimal values using the least error square method). Moreover, the optimal values for the uncertain parameters can be found individually, unlike those from the least error square method. It is also found that the measurement points should not be located at the nodal points of the dominant acoustic modes; otherwise, the identification process becomes unidentifiable. For cases in which large modal truncation errors (or modeling errors) exist, the identification process also becomes unidentifiable.

1. Introduction

In practice, the sound pressure distribution within an enclosed space is important for interior acoustic design. To obtain the continuous sound pressure distribution without many measurement points, a model must be set up and values assigned to the model parameters. Hence, the assigned values are the key factors in achieving accurate predictions. This paper proposes the use of a probabilistic approach to calculating the optimal values assigned to the model parameters by utilizing a few measurement points.

Many researchers (e.g. Pretlove [1], Dowell et al. [2], and Narayanan and Shanbhag [3]) have theoretically developed sound pressure models within rectangular enclosed spaces. Most of them have adopted classical approaches to solving the wave equation that is associated with the boundary conditions to obtain the sound pressure distribution function. Jackson [4], Oldham and Hillarby [5], and Pan et al. [6] studied similar

*Corresponding author.
E-mail address: bcraylee@cityu.edu.hk (Y.Y. Lee).

0022-460X/$ - see front matter © 2006 Elsevier Ltd. All rights reserved.
doi:10.1016/j.jsv.2006.05.040

problems experimentally and theoretically. They found that the values assigned to the modal parameters were not accurate due to uncertain boundary conditions or damping factor or other parameters, which resulted in poor prediction at low frequencies. This is also a common problem in structural modeling, but it can be solved using system identification methods to obtain the optimal model parameters for the best prediction. This paper introduces a framework for probabilistic system identification and incorporates it into the acoustic model to solve the uncertain parameters.

Few research works have been directly related to the problem in this paper. Some previous works on the identification of an acoustic model from measured responses are as follows. Mckelvey et al. [7] proposed the subspace system identification method to obtain the acoustic model of a regular duct using the measured responses. Henry and Clark [8] and Clark and Fuller [9] set up the transfer functions for particular inputs and outputs in their acoustic models and used them in the control design schemes. The model could only predict the responses at the output locations. These identification processes were mainly used for active control, which is different from the main theme of this paper (which can predict the response of any location, once the uncertain parameters are identified). Other research groups, such as those of Choi and Kim [10], Kim and Nelson [11], Williams [12], Maynard and Veronesi [13] developed various methodologies to reconstruct the sound pressures that are radiated from sources under a free field condition or identify their numbers and locations. Unlike the focuses in these studies, however, any uncertain parameters in the room model of this paper can be identified using the proposed probabilistic method. The acoustic model input with the identified parameters is used for sound pressure prediction.

System identification is a ''non-unique'' inverse problem with uncertainties in the identified results. To handle the ''non-uniqueness'' problem and properly describe the ''uncertainties'', probabilistic methods should be employed. Instead of pinpointing one solution of the model parameters, probabilistic system identification methods focus on the calculation of the probability density function (PDF) for the uncertain parameters. One outstanding advantage of the Bayesian statistical identification framework is that engineering judgments can be easily incorporated into the analysis to reduce the uncertainties of the identification results. Beck [14] discovered the PDF of the uncertain model parameters in the measure-of-fit function peak at some optimal points, provided that the number of available data points was very large and the modeling and measurement errors were relatively small. Based on asymptotic approximation [15,16], Beck and Katafygiotis proposed to approximate this PDF by a weighted sum of Gaussian distributions that was centered at these optimal points. The task of finding all global maxima of the measure-of-fit function is non-trivial, and can be effectively handled by the algorithm presented in Ref. [16]. This development was a milestone in the Bayesian system identification framework. It is one of the objectives of this paper to extend this framework and apply it in updating acoustic model parameters.

2. Theory

2.1. Acoustic model

The model of a rectangular enclosed space with air leakages M_p, is presented in this sub-section. In Fig. 1, the acoustic velocity potential within the rectangular room subject to a steady-state uniform distributed sound pressure is given by the following homogeneous wave equation [17]:

$$\nabla^2\phi - \frac{1}{c^2}\frac{\partial^2\phi}{\partial t^2} = 0, \tag{1}$$

where ϕ is the velocity potential function and c is the speed of sound.

The air particle velocities in the x, y, and z directions and pressures within the air cavity are given by $\partial\phi/\partial x$, $\partial\phi/\partial y$, $\partial\phi/\partial z$, and $-\rho(\partial\phi/\partial t)$, respectively, where ρ is the air density.

The boundary conditions of the rectangular cavity to be satisfied are

$$\left.\frac{\partial\phi}{\partial x}\right|_{x=0} = \left.\frac{\partial\phi}{\partial x}\right|_{x=L_x} = 0; \quad \left.\frac{\partial\phi}{\partial y}\right|_{y=0} = \left.\frac{\partial\phi}{\partial y}\right|_{y=L_y} = 0, \tag{2a,b}$$

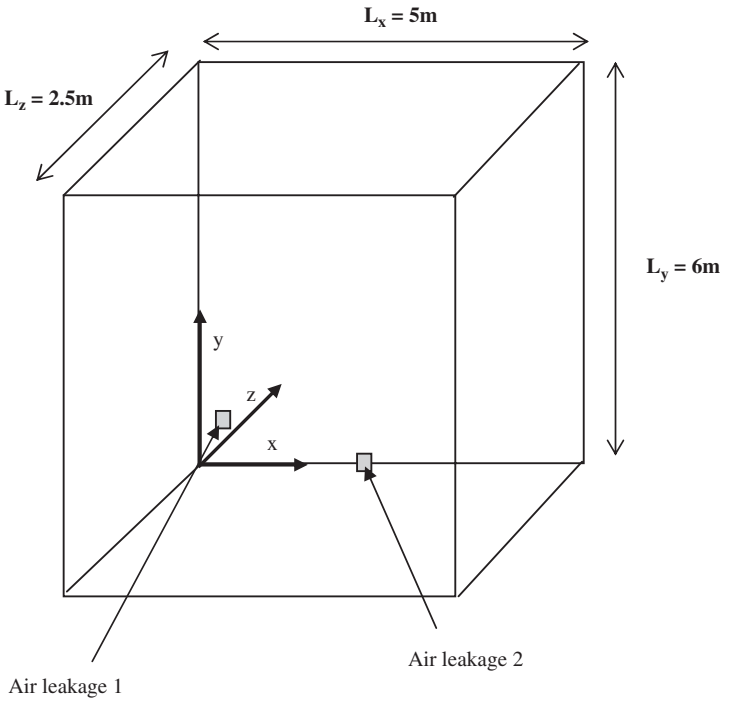

Fig. 1. Theoretical model of a room with two air leakages.

$$\left.\frac{\partial\phi}{\partial z}\right|_{z=0} = 0; \quad \left.\frac{\partial\phi}{\partial z}\right|_{z=-L_z} = v(x,y,t), \tag{2c,d}$$

where L_x, L_y, and L_z are the dimensions of the room, and $v(x,y,t)$ is the velocity at $z=-L_z$.

$f_o(t)=f_o e^{i\omega t}$ is the external steady-state sound pressure. $v(x,y,t)$ can be expressed as $v(x,y)e^{i\omega t}$, i is the complex number $\sqrt{-1}$, and ω is the frequency in radian/s. In Fig. 1, it is assumed that the two air leakages are located at $x_1 \leqslant x \leqslant x_1 + L'_{x_1}$, $y_1 \leqslant y \leqslant y_1 + L'_{y_1}$ and $x_2 \leqslant x \leqslant x_2 + L'_{x_1}$, $y_2 \leqslant y \leqslant y_2 + L'_{y_1}$, respectively. L'_{x_1}, L'_{x_2}, L'_{y_1}, and L'_{y_2} are the widths and lengths of the air leakages. The velocity profiles at the air leakages are assumed to be double the sine function. Thus, the particle velocity profile at $z=-L_z$ is given by

$$v(x,y) = \begin{cases} i\omega A_1 \sin\left(\frac{\pi(x-x_1)}{L'_{x_1}}\right)\sin\left(\frac{\pi(y-y_1)}{L'_{y_1}}\right) & \text{for air leakage 1,} \\ i\omega A_2 \sin\left(\frac{\pi(x-x_2)}{L'_{x_2}}\right)\sin\left(\frac{\pi(y-y_2)}{L'_{y_2}}\right) & \text{for air leakage 2,} \\ 0 & \text{for the rigid wall,} \end{cases} \tag{3}$$

where A_1 and A_2 are the air particle displacement amplitudes at the leakages.

By applying the boundary conditions in Eq. (2a–d), the solution of Eq. (1) can be expressed [1,17–19] as

$$\phi(x,y,z,t) = i\omega e^{i\omega t}\sum_{n=0}^{N}\sum_{m=0}^{M}\frac{(A_1\alpha_{1,nm}+A_2\alpha_{2,nm})\cosh(\mu_{nm}z)}{\mu_{nm}\sinh(\mu_{nm}L_z)}\cos\left(\frac{n\pi x}{L_x}\right)\cos\left(\frac{m\pi y}{L_y}\right), \tag{4}$$

where $\mu_{nm}=\sqrt{\omega_{nm}^2-\omega^2}/c$, $\omega_{nm}^2=c^2\pi^2[(n/L_x)^2+(m/L_y)^2]$, for a damped system it is assumed that $\mu_{nm}=\sqrt{\omega_{nm}^2+\xi\omega\omega_{nm}-\omega^2}/c$, ξ is the damping ratio, N and M are the numbers of the acoustic modes used in the x and y directions, respectively, $\alpha_{1,nm}$ and $\alpha_{2,nm}$ are the modal coupling coefficients depending on

the locations and sizes of the air leakages and the corresponding acoustic modes, as given below:

$$\alpha_{1,nm} = \frac{\int_{S_1} \sin\left(\frac{\pi(x-x_1)}{L'_{x_1}}\right) \sin\left(\frac{\pi(y-y_1)}{L'_{y_1}}\right) \cos\left(\frac{n\pi x}{L_x}\right) \cos\left(\frac{m\pi y}{L_y}\right) \mathrm{d}S}{\int_{S_1} \cos\left(\frac{n\pi x}{L_x}\right)^2 \cos\left(\frac{m\pi y}{L_y}\right)^2 \mathrm{d}S}, \tag{5a}$$

$$\alpha_{2,nm} = \frac{\int_{S_2} \sin\left(\frac{\pi(x-x_2)}{L'_{x_2}}\right) \sin\left(\frac{\pi(y-y_2)}{L'_{y_2}}\right) \cos\left(\frac{n\pi x}{L_x}\right) \cos\left(\frac{m\pi y}{L_y}\right) \mathrm{d}S}{\int_{S_2} \cos\left(\frac{n\pi x}{L_x}\right)^2 \cos\left(\frac{m\pi y}{L_y}\right)^2 \mathrm{d}S}, \tag{5b}$$

where $S_1 = L'_{x_1} L'_{y_1}$ and $S_2 = L'_{x_2} L'_{y_2}$ are the leakage areas.

The internal sound pressure force is equal to $-\rho(\partial\phi/\partial t)$, and is given by

$$f(x, y, \omega, t) = \mathrm{e}^{\mathrm{i}\omega t} H(x, y, -L_z, \omega), \tag{6}$$

where

$$H(x, y, z, \omega) = \rho\omega^2 \sum_{n=0}^{N} \sum_{m=0}^{M} \frac{(A_1\alpha_{1,nm} + A_2\alpha_{2,nm}) cosh(\mu_{nm} z)}{\mu_{nm} \sinh(\mu_{nm} L_z)} \cos\left(\frac{n\pi x}{L_x}\right) \cos\left(\frac{m\pi y}{L_y}\right).$$

Consider the resulting differential equation for the average displacements at the air leakages [13]:

$$m \frac{\mathrm{d}^2\bar{w}_1}{\mathrm{d}t^2} + R_1 \frac{\mathrm{d}\bar{w}_1}{\mathrm{d}t} = \bar{f}_1(t) - f_o(t), \tag{7a}$$

$$m \frac{\mathrm{d}^2\bar{w}_2}{\mathrm{d}t^2} + R_2 \frac{\mathrm{d}\bar{w}_2}{\mathrm{d}t} = \bar{f}_2(t) - f_o(t), \tag{7b}$$

where $m = \rho h$, $R_1 = \rho c k^2 S_1(2\pi)$, and $R_2 = \rho c k^2 S_2(2\pi)$ are the equivalent air mass and sound radiation impedance at the leakages, respectively [20], h is the wall thickness, $k = \omega/c$ is the wavenumber, and $\bar{w}_1$, $\bar{w}_2$, $\bar{f}_1$, and $\bar{f}_2$ are the average air particle displacement and internal sound pressure forces, which are given as

$$\bar{w}_1(t) = A_1 \mathrm{e}^{\mathrm{i}\omega t} \frac{\int_{S_1} \sin(\pi(x-x_1)/L'_{x_1}) \sin(\pi(y-y_1)/L'_{y_1}) \mathrm{d}S}{S_1} = A_1 \mathrm{e}^{\mathrm{i}\omega t} \left(\frac{2}{\pi}\right)^2, \tag{8a}$$

$$\bar{f}_1 = \rho\omega^2 \mathrm{e}^{\mathrm{i}\omega t} \sum_{n=0}^{N} \sum_{m=0}^{M} \frac{(A_1\alpha_{1,nm} + A_2\alpha_{2,nm})}{\mu_{nm} \tanh(\mu_{nm} L_z)} \beta_{1,nm}. \tag{8b}$$

Similarly,

$$\bar{w}_2(t) = A_2 \mathrm{e}^{\mathrm{i}\omega t} \left(\frac{2}{\pi}\right)^2, \tag{9a}$$

$$\bar{f}_2 = \rho\omega^2 \mathrm{e}^{\mathrm{i}\omega t} \sum_{n=0}^{N} \sum_{m=0}^{M} \frac{(A_1\alpha_{1,nm} + A_2\alpha_{2,nm})}{\mu_{nm} \tanh(\mu_{nm} L_z)} \beta_{2,nm}, \tag{9b}$$

where

$$\beta_{1,nm} = \frac{\int_{S_1} \cos\left(\frac{n\pi x}{L_x}\right) \cos\left(\frac{m\pi y}{L_y}\right) \mathrm{d}S}{S_1} \quad \text{and} \quad \beta_{2,nm} = \frac{\int_{S_1} \cos\left(\frac{n\pi x}{L_x}\right) \cos\left(\frac{m\pi y}{L_y}\right) \mathrm{d}S}{S_2}.$$

By substituting Eqs. (8a), (8b, (9a) and (9b) into Eqs. (7a) and (7b), the displacement amplitudes A_1 and A_2 can be obtained. The sound pressure distribution in dB scale for all frequency components of the

excitation is defined by

$$\mathrm{SPL}(x,y,z) = 10\log\left[\int_{\omega_l}^{\omega_u} \left|H(x,y,z,\omega)\right|^2 \mathrm{d}\omega\right], \tag{10}$$

where ω_l and ω_u are the lower and upper cutoff frequencies of the random excitation, respectively. The sound pressure in the time domain can be derived using the inverse Fourier transform method.

2.2. Proposed probabilistic approach

The probabilistic identification framework [15,16,21,22], which was originally employed in structural model updating and health monitoring, is extended in this paper for the identification of the uncertain parameters of an acoustic model to reconstruct the interior sound pressure of the system. Unlike the deterministic approach, the probabilistic approach aims to calculate the posterior (updated) PDF of the uncertain parameters for a given set of measurement data. In this study, we define $\boldsymbol{\theta} = \{\mathbf{a}^{\mathrm{T}}\sigma\}^{\mathrm{T}}$ as the uncertain parameter vector to be updated, where $\mathbf{a}$ contains the leakage locations (x_1, y_1) and (x_2, y_2) and the corresponding leakage sizes S_1 and S_2. σ represents the prediction error which is defined as the difference between the measured output and input. Herein, the assumption is made that the prediction error is both spatially and temporally independent and normally distributed. The measurement data D_N includes the interior sound pressure and external sound pressure, which are the output and input data in the probabilistic identification model. Based on the Bayes' Theorem, the posterior PDF of $\boldsymbol{\theta}$ for a given set of measured sound pressure data D_N can be expressed by

$$p(\boldsymbol{\theta}|D_N, M_P) = \frac{p(D_N|\boldsymbol{\theta}, M_P)p(\boldsymbol{\theta}|M_P)}{p(D_N|M_P)}, \tag{11}$$

where $p(\boldsymbol{\theta}|M_P) = \pi(\boldsymbol{\theta})$ is the prior PDF of $\boldsymbol{\theta}$, which allows judgment about the relative plausibility of the values of $\boldsymbol{\theta}$ to be considered. M_p represents the classical acoustic model developed in Section 2.1. The PDF of obtaining the set of measured sound pressure data D_N for a given M_P can be expressed as

$$p(D_N|M_P) = \int_{S(\boldsymbol{\theta})} p(D_N|\boldsymbol{\theta}, M_P)p(\boldsymbol{\theta}|M_P)\,\mathrm{d}\boldsymbol{\theta} = c^{-1}. \tag{12}$$

Therefore, Eq. (11) can be expressed as

$$p(\boldsymbol{\theta}|D_N, M_P) = cp(D_N|\boldsymbol{\theta}, M_P)\pi(\boldsymbol{\theta}), \tag{13}$$

where c is a normalizing constant. The most important term in Eq. (13) is $p(D_N|\boldsymbol{\theta}, M_P)$, which is the contribution of the measured sound pressure data in the posterior PDF, and is given by

$$p(D_N|\boldsymbol{\theta}, M_P) = \frac{1}{\left(\sqrt{2\pi}\sigma\right)^{NN_o}} \exp\left[-\frac{1}{2\sigma^2}\sum_{n=1}^{N}\left\|\hat{\mathbf{q}}(n) - \mathbf{q}(n;\mathbf{a})\right\|^2\right], \tag{14a}$$

where N_O is the number of measurement stations, N the number of measured time steps at each measurement station, $\hat{q}(n)$ the vector of measured sound pressures at the nth time step, $\mathbf{q}(n;\mathbf{a})$ the vector of calculated sound pressures based on the model M_P for a given set of uncertain parameters $\mathbf{a}$, and $\|\cdot\|$ is the usual Euclidean norm of a vector.

The uncertainty in the acoustic model parameters is quantified by the marginal distribution of $\mathbf{a}$. The posterior marginal PDF of the acoustic parameters $\mathbf{a}$ can be obtained from Eq. (13) by integrating over σ as follows:

$$p(\mathbf{a}|D_N, M_P) = \int_0^{\infty} cp(D_N|\mathbf{a}, \sigma, M_P)\pi(\mathbf{a}, \sigma)\,\mathrm{d}\sigma. \tag{14b}$$

Assuming that the prior distribution $\pi(\mathbf{a}, \sigma)$ is a slowly varying function of σ and that the number N of measured data is sufficiently large, it can be shown that the integrand in the right hand side of Eq. (14b)

generally peaks at the optimal values of the $J(\mathbf{a})$ function as defined below:

$$J(\mathbf{a}) = \frac{1}{NN_O} \sum_{n=1}^{N} \left\| \hat{\mathbf{q}}(n) - \mathbf{q}(n;\mathbf{a}) \right\|^2 = \hat{\sigma}^2(\mathbf{a}). \tag{14c}$$

More details about Eq. (14c) are shown in Appendix A. This positive definite measure-of-fit function between the measured and modeled sound pressures $J(\mathbf{a})$ is equal to $\hat{\sigma}^2(\mathbf{a})$, which represents the optimal variance in the prediction error model. The integral in Eq. (14b) can then be calculated using an asymptotic approximation that is available for this type of integral [24], resulting in

$$p(\mathbf{a}|D_N, M_P) = c_1 J(\mathbf{a})^{-N_J} \pi(\mathbf{a}, \hat{\sigma}(\mathbf{a})). \tag{15a}$$

For non-informative (uniform) prior distribution π,

$$p(\mathbf{a}|D_N, M_P) = c_1 J(\mathbf{a})^{-N_J}, \tag{15b}$$

where c_1 is a normalizing constant so that the integration of the term on the right-hand side of Eq. (15) over the pre-defined domain is equal to unity, and $N_J = (NN_O - 1)/2$; N and N_O are the numbers of measured time steps and measurement locations, respectively; $J(\mathbf{a})$ and $\hat{\sigma}(\mathbf{a})$ are defined in Eq. (14b); $\pi(a,\sigma)$ is the prior PDF of the uncertain parameters. The posterior PDF for particular uncertain parameters $\boldsymbol{a}^*$ is given by

$$p(\mathbf{a}^*|D_N, M_P) = \int_{S(\mathbf{a}')} p(\mathbf{a}|D_N, M_P)\, \mathrm{d}\mathbf{a}', \tag{16}$$

where $\mathbf{a}'$ is the uncertain parameter vector excluding $\boldsymbol{a}^*$.

The posterior PDF in Eq. (15) gives the plausibility of the acoustic model parameter values over the domain $S(\mathbf{a})$ after updating. In practice, the exponent N_J in Eq. (15a) is a large number, and the relatively posterior probabilities of the various acoustic model parameters $\mathbf{a}$ are very sensitive to the corresponding values of $J(\mathbf{a})$. In such a situation, there is a finite number of optimal points $\hat{\mathbf{a}}^{(k)}$, for $k = 1, \ldots, K$, that satisfy

$$J\left(\hat{\mathbf{a}}^{(k)}\right) = \min_{\mathbf{a} \in S(\mathbf{a})} J(\mathbf{a}) = \hat{\sigma}^2. \tag{17}$$

Model updating problems in such situations can be classified as identifiable cases [15,16]. When the number N is not large and/or the location of measurement station is not informative, it is possible for model updating problems to fall into the unidentifiable cases [21,23]. It must be pointed out that the treatments of model updating problems in unidentifiable cases are much more complex than those in the identification cases. This paper focuses only on acoustic model updating problems under the identifiable catalog.

In the identifiable cases, the posterior PDF of the model parameters $\mathbf{a}$ in Eq. (15) can be asymptotically approximated [15,16] as

$$p(\mathbf{a}|D_N, M_P) \approx \sum_{k=1}^{K} w_k \mathbf{N}\left(\hat{\mathbf{a}}^{(k)}, A_N^{-1}\left(\hat{\mathbf{a}}^{(k)}\right)\right), \tag{18}$$

where $\mathbf{N}(\boldsymbol{\mu}, \boldsymbol{\Sigma})$ denotes a multivariate Gaussian distribution with mean $\boldsymbol{\mu}$ and covariance matrix $\boldsymbol{\Sigma}$, $A_N(\mathbf{a})$ is the Hessian of the function $g(\mathbf{a}) = N_J \ln J(\mathbf{a})$, and w_k is the weighting coefficients and is given by

$$w_k = \frac{w_k'}{\sum_{k=1}^{k} w_k'} \quad \text{where} \quad w_k' = \pi\left(\hat{\mathbf{a}}^{(k)}\right) \left| A_N\left(\hat{\mathbf{a}}^{(k)}\right) \right|^{-1/2}. \tag{19}$$

Eq. (18) implies that the posterior PDF of the acoustic model parameters $\mathbf{a}$ can be approximated as a finite weighted sum of Gaussian distributions that is centered at the optimal points $\hat{\mathbf{a}}^{(k)}$, for $k = 1, \ldots, K$. It must be pointed out that the task of finding all global minima of the non-convex function $J(\mathbf{a})$ in Eq. (14c) is non-trivial. Katafygiotis and Beck [16] presented an algorithm for identifiable cases that finds all output-equivalent optimal parameters once one of them is given. The posterior PDF of the predicted interior sound pressure at any point can be approximated by the method that is presented in Ref. [22]. Unlike the deterministic approach, which aims at pin-pointing a solution, the probabilistic approach calculates the posterior PDF of the uncertain parameters and the predicted responses of the system. In this paper, the most commonly used

deterministic method, the least error square method [25], is used to demonstrate the difference between the probabilistic and deterministic approaches in the system identification of the acoustic model and the reconstruction of the interior sound pressure of a room.

3. Numerical simulations

A rectangular enclosed room that is subjected to a uniform random sound pressure is used as a verification example (see Fig. 1). The dimensions of the room are $2.5\,\mathrm{m} \times 5\,\mathrm{m} \times 6\,\mathrm{m}$, and the thicknesses of all walls are equal to 10 cm. Two square leakages with sizes $0.25\,\mathrm{m} \times 0.25\,\mathrm{m}$ and $0.2\,\mathrm{m} \times 0.2\,\mathrm{m}$ are located at the coordinates (2.1 m, 2.52 m, −2.5 m) and (3 m, 1.92 m, −2.5 m) of the room, respectively, as shown in Fig. 1. The system is assumed to be classically damped with a damping ratio of $\xi = 0.01$ in the simulation. Only the lowest 6 acoustic modes are considered. The lowest and highest non-zero resonant frequencies are 34.3 and 66.7 Hz, respectively. The frequency range of the external sound pressure is from 20 to 80 Hz. Measurement noise is simulated by adding a 5% white noise to the calculated time-domain responses. A simulation of 0.8 s is used in the identification process with a time step of 0.0125 s. A non-informative (uniform) prior distribution π is employed in the calculation of the normalized PDF in the following three cases (see Fig. 1).

1. *Case* I: 2 square leakages are considered in this case. The uncertain parameter vector $\mathbf{a} = \left\{x_1, y_1, x_2, y_2, L'_{x_1}, L'_{x_2}\right\}$ consists of the leakage locations (x_1, y_1, and x_2, y_2) and sizes ($L'_{x_1} = L'_{y_1}$ and $L'_{x_2} = L'_{y_2}$). The 2 internal sound pressure measurement stations are located at (1 m, 4.3 m, 1.75 m) and (3.5 m, 1.2 m, 0.5 m). One external sound measurement is used for the identification process. This case is used for the comparison between the proposed probabilistic method and the least error square deterministic method.
2. *Case* II: This is the same as *Case* I except that the two internal sound pressure measurement stations are located at (2.5 m, 3 m, 1.75 m) and (2.5 m, 3 m, 0.5 m). This case allows for studying the effect of measurement locations on the results of system identification.
3. *Case* III: This is the same as *Case* I except that the number of the acoustic modes used in the analysis is smaller than that in the simulation. This case allows for the studying of modeling error.

3.1. Case I: comparison of the proposed and least error square methods

First, *Case* I is considered. The square of the normalized prediction error is plotted against different leakage locations in Fig. 2a. The square of the prediction error is normalized such that the maximum value is equal to unity. Fig. 2b shows the 36 leakage locations that are considered in Fig. 2a on the surface $z = -L_z$. It is assumed that both leakages are located on this surface. In Fig. 2a, there are many local peaks, at which the prediction errors are very similar to each other and are all very close to the global minimum. In such a situation, it is very easy for the numerical optimization algorithm to be trapped at the regions of local minimum. That is, optimizations with different initial trials will very likely to result in different solutions. By following a deterministic approach, it is not possible to make any reasonable conclusions.

Fig. 2c shows the square of the prediction error as a function of the leakage sizes. The values of the normalized prediction error square are almost the same at the region for the leakage 1 and 2 sizes that vary from 2 to 8 cm. In fact, the prediction error for points on the dashed line in Fig. 2c are very close to the global minimum. Note that the acoustic model is parameterized by more than two parameters (e.g., the x and y coordinates of the first and second leakages, and the corresponding sizes); however, at most two parameters can be pointed in one three-dimensional figure. In Figs. 2a and c, the parameters that are not shown in the figure are at the corresponding optimal values.

Next, the proposed probabilistic method is employed in handling the same problem (*Case* I). Different projections of the normalized PDF are show in Figs. 2d–f. Unlike Figs. 2a and c, there is only one sharp peak in the domain of interest in Figs. 2d–f. Based on the results of Figs. 2d–f, it can be concluded that the region of

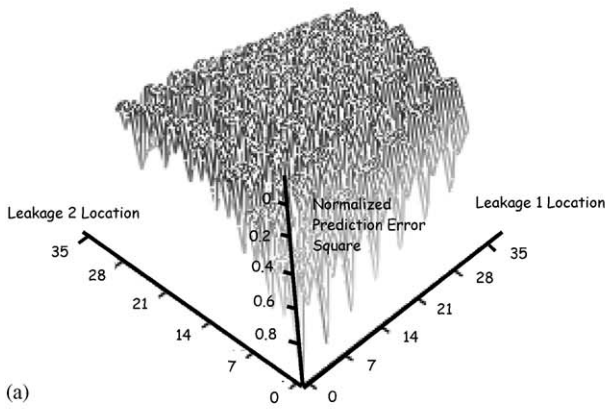

(a)

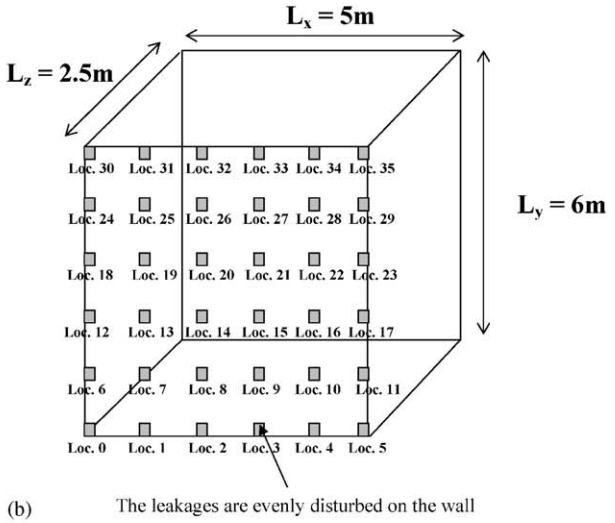

(b)

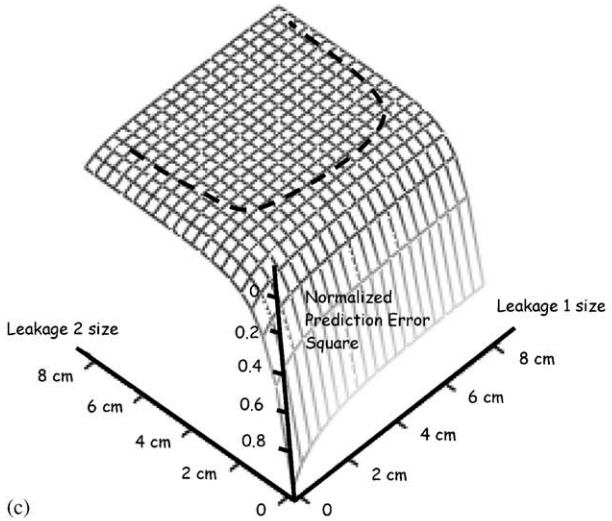

(c)

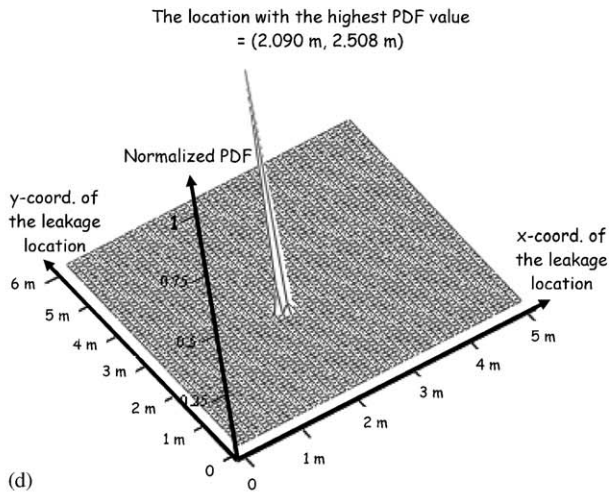

(d)

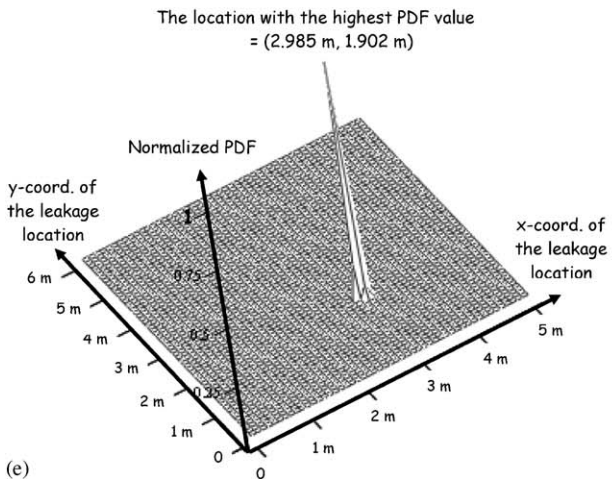

(e)

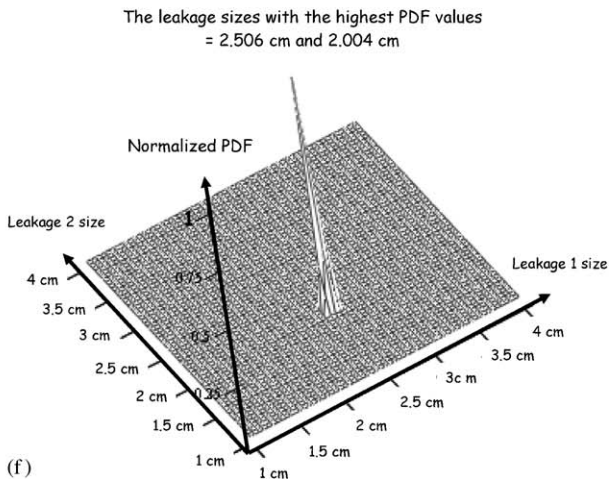

(f)

Fig. 2. (a) Normalized prediction error square for different leakage locations (sizes of leakages 1 and $2 = 0.025\,\text{m} \times 0.025\,\text{m}$ and $0.02\,\text{m} \times 0.02\,\text{m}$), (b) leakage locations from 0 to 35 on the surface $z = -L_z$, (c) normalized prediction error square for different leakage sizes (leakage locations = (3 m, 1.6 m, −2.5 m) and (2.1 m, 2.1 m, −2.5 m)), (d) normalized PDF vs. the location of air leakage 1, (e) normalized PDF vs. the location of air leakage 2, (f) normalized PDF vs. the two leakage sizes.

high probability concentrates in the neighborhoods of the optimal point

$$\mathbf{a} = \left\{x_1, y_1, x_2, y_2, L'_{x_1}, L'_{x_2}\right\} = \{2.090\,\text{m}, 2.508\,\text{m}, 2.985\,\text{m}, 1.902\,\text{m}, 2.506\,\text{cm}, 2.004\,\text{cm}\}.$$

The true value is {2.1 m, 2.52 m, 3 m, 1.92 m, 2.5 cm, 2.0 cm}, which is slightly different from the identified value due to the introduction of 5% measurement noise. From Figs. 2d–f, it can be observed that the PDF

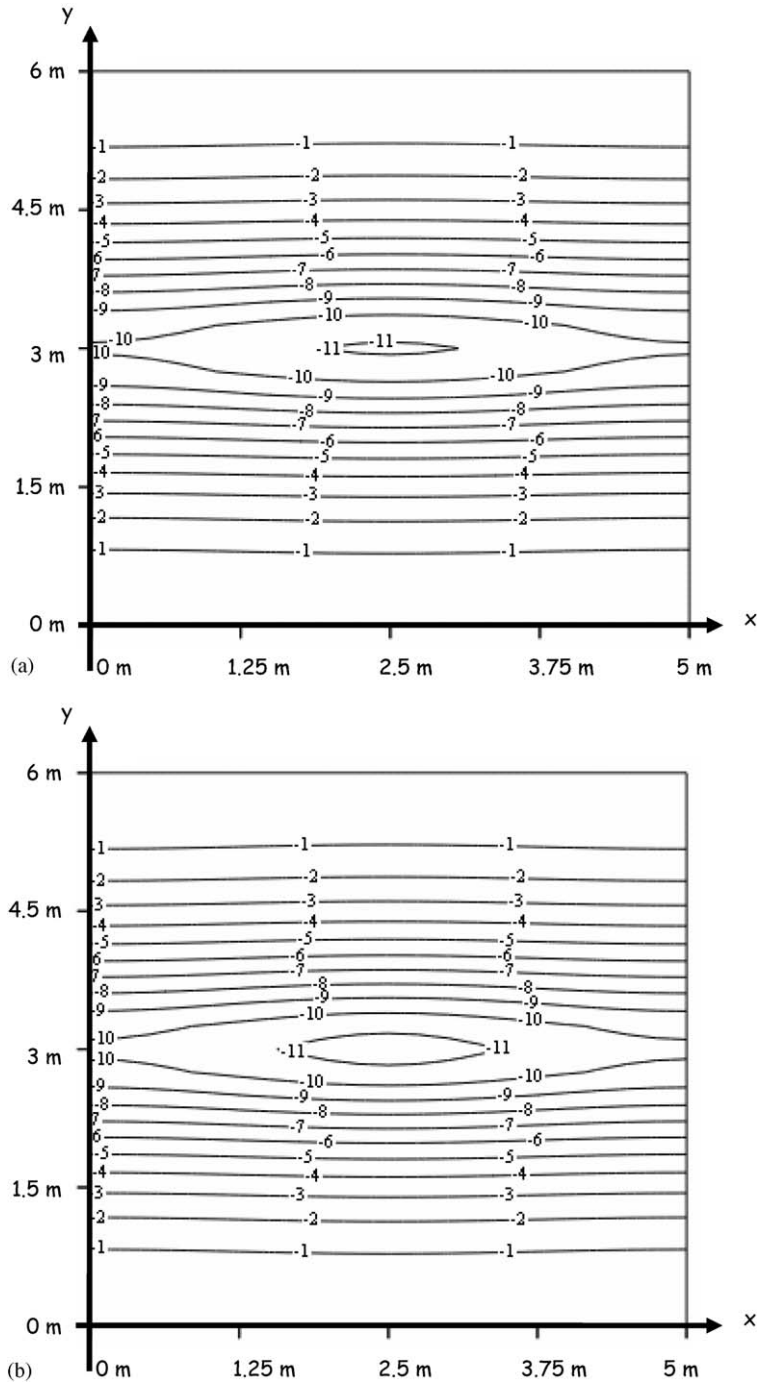

Fig. 3. (a) Original sound pressure distribution in dB scale, (b) reconstructed sound pressure distribution in dB scale.

value decays rapidly in all directions away from the optimal point. This clearly shows that model updating in *Case* I is identifiable based on the definition given in Ref. [23].

The interior sound pressure distribution at $z = 0$ is reconstructed based on the identified acoustic model using the proposed probabilistic method, and is plotted in Fig. 3b. The interior sound pressure is normalized to ensure that the maximum value equals 0 dB. Fig. 3a shows the original sound pressure distribution at the same location ($z = 0$). By comparing Figs. 3a and b, it can be concluded that the original and re-constructed sound pressure distributions are closely matched, because the identified acoustic model parameters are very close to the true values.

3.2. Case II: effect of measurement locations

In *Case* II, the measurement stations are located at the nodal points of the (1,0), (0,1), and (1,1) acoustic modes, which have significantly contribution to the overall sound pressure responses. Therefore, the measured sound pressure that is employed in the identification process in this case is not as sensitive as that in *Case* I. Different projections of the normalized PDF are summarized in Figs. 4a–c.

Considering Fig. 4c, a sharp peak can be identified as in *Case* I, showing that the leakage sizes in *Case* II is still identifiable. However, when Fig. 4a is considered, the normalized PDF values for all points along the line

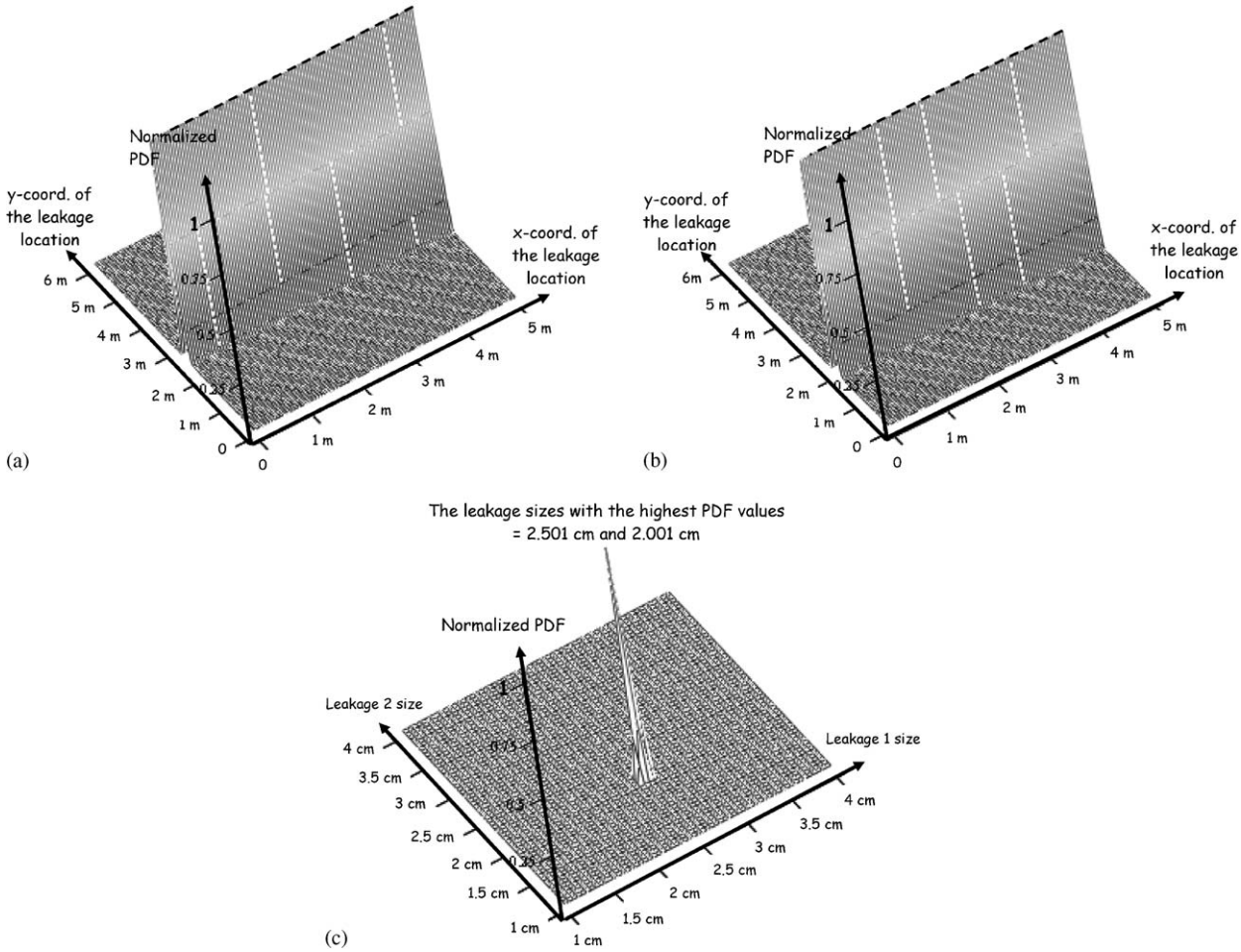

Fig. 4. (a) Normalized PDF vs. the location of air leakage 1 (measurement stations located at the nodal points), (b) normalized PDF vs. the location of air leakage 2 (measurement stations located at the nodal points), (c) normalized PDF vs. the two leakage sizes (measurement stations located at the nodal points).

$y_1 = 2.503$ within the domain of interest are exactly the same. In this case, the set of optimal points corresponds to a straight line in the parameter space, and the posterior PDF of the parameters is concentrated in the neighborhood of this line, instead of being concentrated in the neighborhood of a single point as in *Case* I. A very similar observation can be made of Fig. 4b, in which the points of high normalized PDF value are concentrated in the neighborhood of the line $y_2 = 1.904$. These show that the updating problem in *Case* II is unidentifiable according to the definition given in Ref. [23]. This is the reason for using Eq. (15) instead of (18) in the calculation of the normalized PDF in this case. Eq. (18) is valid only for identification cases. It must be pointed out that the computational power and time required for using Eq. (18) is much lower than that for Eq. (15). For model updating problems with more uncertain parameters, it is computationally prohibitive to use Eq. (15). Several computationally efficient numerical algorithms for approximating the posterior PDF in the general unidentifiable cases are available in Refs. [21,23]. The measurement stations should be set at non-nodal points of the dominant modes to avoid unidentifiable model updating problems.

3.3. Case III: effect of modal truncation error

Case III, which consists of two parts, focuses on the effect of the modeling error of the prediction model. The lowest 6 modes are employed in the simulation model while only 4 and 2 modes are considered in the prediction models in *Cases* IIIa and IIIb, respectively.

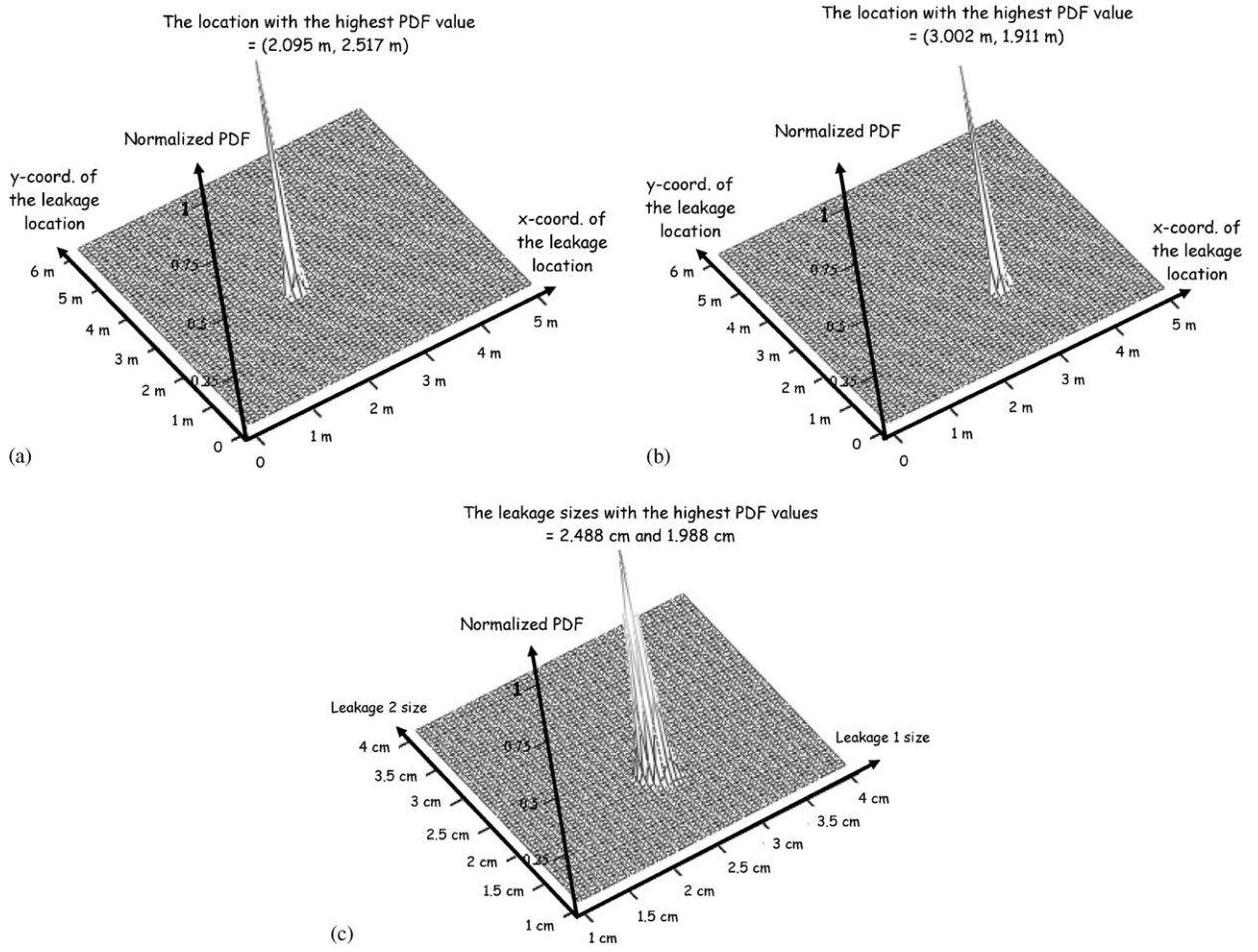

Fig. 5. (a) Normalized PDF vs. the location of air leakage 1 (4 modes used), (b) normalized PDF vs. the location of air leakage 2 (4 modes used), (c) normalized PDF vs. the two leakage sizes (4 modes used).

Firstly, only the lowest 4 acoustic modes are considered in the prediction model. These 4 modes have dominant contributions to the overall sound pressure responses of the system. Figs. 5a–c show the projections of the calculated normalized PDF within the domain of interest. A single peak can be identified in each of the three figures, and the identified optimal point {2.095 m, 2.517 m, 3.002 m, 1.911 m, 2.488 cm, 1.988 cm} is close to the true value.

In Fig. 5c, the decay of the PDF value away from the optimal point is slower than that in Fig. 2f (or the peak in Fig. 5c is not as sharp as that in Fig. 2f). This implies that the uncertainty in *Case* IIIa is higher than that in *Case* I.

Fig. 6 shows the reconstructed interior sound pressure distribution at $z = 0$, which is slightly different from that in Fig. 3a, especially around the center of the area. This occurs because only 4 modes are used in the sound pressure reconstruction.

Finally, *Case* IIIb is performed, in which only the lowest 2 acoustic modes are employed in the prediction model. The modeling error in this case is relatively large when compared to that in *Case* IIIa. Based on Eq. (15), the normalized PDF is calculated and summarized in Figs. 7a–c. From Figs. 7a to b, it is clear that the model updating problem in *Case* IIIb is unidentifiable. The situation is very similar to that in *Case* II. Although a peak can be identified in Fig. 7c, the decay of the PDF value away from the optimal point is much slower than that in *Cases* IIIa and I (see Fig. 6c and Fig. 2f). It can be concluded that the uncertainty associated with the acoustic parameters **a** is much higher in this case than in *Cases* IIIa and I.

4. Conclusions

This paper puts forward a new methodology for the reconstruction of interior sound pressure from an acoustic model, in which some model parameters are uncertain. The model considered is a rectangular room with two air leakages, and the room is subjected to external random noise. To reconstruct the interior sound pressure, the probabilistic system identification framework, which was originally used in structural model updating and health monitoring, is used to obtain the posterior PDF of the set of uncertain acoustic model parameters based on a given set of measured sound pressure. Unlike the least error square method (the most

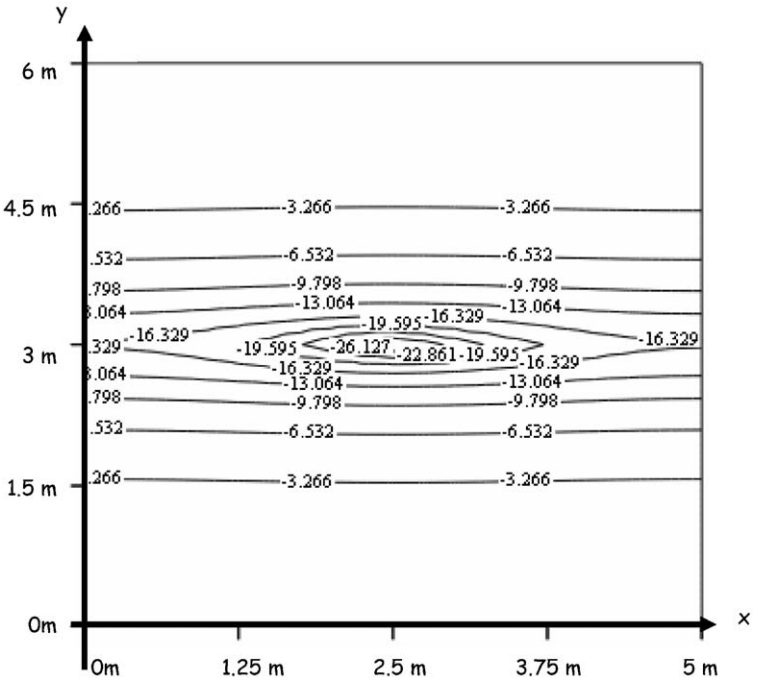

Fig. 6. Reconstructed sound pressure distribution in dB scale (4 modes used).

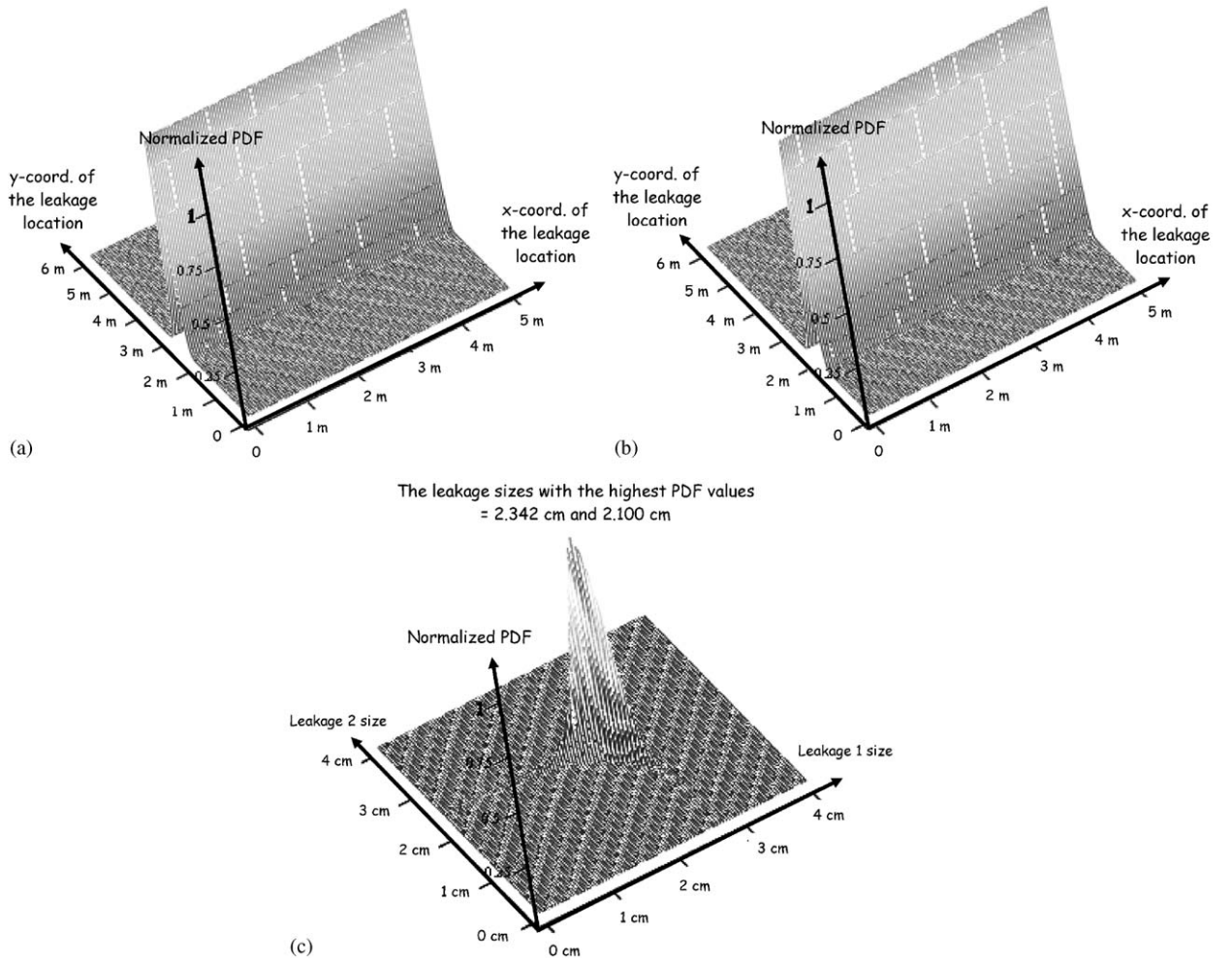

Fig. 7. (a) Normalized PDF vs. the location of air leakage 1 (2 modes used), (b) normalized PDF vs. the location of air leakage 2 (2 modes used), (c) normalized PDF vs. the two leakage sizes (2 modes used).

common deterministic approach), the proposed probabilistic methodology performs the parameter identification process based on the highest probability of the set of uncertain parameters. The numerical case studies clearly show the superior performance of the proposed probabilistic methodology in the reconstruction of the interior sound pressure.

As the number of the uncertain parameters involved in the acoustic model is small and the number of measured data points available is usually large, this type of system identification problems usually falls into the category of identifiable cases. The numerical case studies show that measurement locations and modeling error have significant effects on the identifiability of the model updating problem. The updating problem will become unidentifiable when the measurement stations are located at the nodal points of the dominant acoustic modes. Enough modes should be considered in the prediction model to avoid unidentifiable cases.

Acknowledgments

The work described in this paper was fully supported by a grant from the Research Grants Council of the Hong Kong Special Administrative Region, China [Project No. 9040798, RGC Ref. No., CityU 1142/03E].

Appendix A

In order to obtain the best model, the posterior PDF of the uncertain parameters $p(\theta|D_N, M_P)$ given by Eq. (13) must be maximized. Consider the logarithm of Eq. (13):

$$\ln p(\boldsymbol{\theta}|D_N, M_P) = \ln c + \ln p(D_N|\boldsymbol{\theta}, M_P) + \ln \pi(\boldsymbol{\theta}). \tag{A.1}$$

From Eq. (14a)

$$\ln p(D_N|\boldsymbol{\theta}, M_P) = -\frac{NN_o}{2}\ln(2\pi) - NN_o \ln \sigma - \frac{1}{2\sigma^2}\sum_{n=1}^{N}\left\|\hat{\mathbf{q}}(n) - \mathbf{q}(n;\mathbf{a})\right\|^2. \tag{A.2}$$

For a given $\mathbf{a}$, maximizing $p(D_N|\boldsymbol{\theta}, M_P)$ with respect to σ requires $\partial \ln p(D_N|\theta, M_P)/\partial\sigma = 0$. If follows:

$$\hat{\sigma}^2(\mathbf{a}) = \frac{1}{NN_o}\sum_{n=1}^{N}\left\|\hat{\mathbf{q}}(n) - \mathbf{q}(n;\mathbf{a})\right\|^2. \tag{A.3}$$

This shows how the most probable variance $\hat{\sigma}^2(\mathbf{a})$, for given $\mathbf{a}$, depends on the choice of the model parameters $\mathbf{a}$. Substituting Eq. (A.3) into Eq. (A.2) yields

$$\ln p\left(D_N|\mathbf{a}, \hat{\sigma}^2(\mathbf{a}), M_P\right) = -\frac{NN_o}{2}\ln(2\pi) - NN_o \ln \hat{\sigma}(\mathbf{a}) - \frac{NN_o}{2}. \tag{A.4}$$

It follows that $p(\boldsymbol{\theta}|D_N, M_P)$ is maximized when $\hat{\sigma}(\mathbf{a})$ is minimized. Thus the most probable model parameters $\mathbf{a}$ are given by minimizing the measure-of-fit function

$$J(\mathbf{a}) = \frac{1}{NN_O}\sum_{n=1}^{N}\left\|\hat{\mathbf{q}}(n) - \mathbf{q}(n;\mathbf{a})\right\|^2 = \hat{\sigma}^2(\mathbf{a}). \tag{A.5}$$

References

[1] A.J. Pretlove, Forced vibration of a rectangular panel backed by a closed rectangular cavity, *Journal of Sound and Vibration* 3 (3) (1966) 252–261.

[2] E.H. Dowell, G.F. Gorman, D.A. Smith, Acoustoelasticity: general theory, acoustic natural modes and forced response to sinuoidal excitation, including comparisons with experiment, *Journal of Sound and Vibration* 52 (4) (1977) 519–542.

[3] S. Narayanan, R.L. Shanbhag, Sound transmission through elastically supported sandwich panels into a rectangular enclosure, *Journal of Sound and Vibration* 77 (2) (1981) 251–270.

[4] R.S. Jackson, Some aspects of the performance acoustic hoods, *Journal of Sound and Vibration* 3 (1) (1966) 82–94.

[5] D.J. Oldham, S.N. Hillarby, The acoustical performance of small close fitting enclosures—part 2: experimental investigation, *Journal of Sound and Vibration* 150 (2) (1991) 261–281.

[6] J. Pan, S.J. Elliott, K.H. Baek, Analysis of low frequency acoustic response in a damped rectangular enclosure, *Journal of Sound and Vibration* 223 (4) (1999) 543–566.

[7] T. McKelvey, A. Fleming, S.O.R. Moheimani, Subspace-based system identification for an acoustic enclosure, *Journal of Vibration and Acoustics* 124 (3) (2002) 414–419.

[8] J.K. Henry, R.L. Clark, Active control of sound transmission through a curved panel into a cylindrical enclosure, *Journal of Sound and Vibration* 249 (2) (2002) 325–349.

[9] R.L. Clark, G.P. Gibbs, C.R. Fuller, An experimental-study implementing model—reference active structural acoustical control, *Journal of the Acoustical Society of America* 93 (6) (1993) 3258–3264.

[10] J. Choi, Y. Kim, Spherical beam-forming and music methods for the estimation of location and strength of spherical sound sources, *Mechanical Systems and Signal Processing* 9 (5) (1995) 569–588.

[11] Y. Kim, P.A. Nelson, Optimal regularization for acoustic source reconstruction by inverse methods, *Journal of Sound and Vibration* 275 (3–5) (2004) 463–487.

[12] E.G. Williams, *Fourier Acoustics: Sound Radiation and Nearfield Acoustical Holography*, Academic Press, New York, 1999.

[13] D.J. Maynard, W.A. Versonesi, Nearfield acoustic holography—II: holographic reconstruction algorithms and computer implementation, *Journal of the Acoustical Society of America* 81 (1978) 1307–1322.

[14] J.L. Beck, Statistical system identification of structures, *Proceedings of the Fifth International Conference on Structural Safety and Reliability* (*ICOSSAR'89*), New York, 1989, pp. 1395–1402.

[15] J.L. Beck, L.S. Katafygiotis, Updating models and their uncertainties: Bayesian statistical framework, *Journal of Engineering Mechanics, ASCE* 124 (4) (1998) 455–461.

[16] L.S. Katafygiotis, J.L. Beck, Updating models and their uncertainties: model identifiability, *Journal of Engineering Mechanics, ASCE* 124 (4) (1998) 463–467.

[17] Y.Y. Lee, Structural–Acoustic Analysis of Close-fitting Enclosures, M. Phil. Thesis, Department of Civil and Structural Engineering, The Hong Kong Polytechnic University, 1995.
[18] Y.Y. Lee, C.F. Ng, The effects of coupled source/cavity modes on the acoustic insertion loss of close-fitting enclosures, *Journal of Building Acoustics* 2 (4) (1997) 549–567.
[19] Y.Y. Lee, C.F. Ng, Sound insertion loss of stiffened enclosure plates using the finite element method and the classical approach, *Journal of Sound and Vibration* 217 (2) (1998) 239–260.
[20] L.E. Kinsler, A.R. Frey, A.B. Coppens, J.V. Sander, *Fundamentals of Acoustics*, fourth ed, Wiley, New York, 2000.
[21] H.F. Lam, Structural Model Updating and Health Monitoring in the Presence of Modeling Uncertainties, PhD Thesis, Department of Civil Engineering, Hong Kong University of Science and Technology, 1999.
[22] L.S. Katafygiotis, C. Papadimitriou, H.F. Lam, A probabilistic approach to structural model updating, *Soil Dynamics and Earthquake Engineering* 17 (7–8) (1998) 495–507.
[23] L.S. Katafygiotis, H.F. Lam, Tangential-projection algorithm for manifold representation in unidentifiable model updating problems, *Earthquake Engineering & Structural Dynamics* 31 (4) (2002) 791–812.
[24] C. Papadimitriou, J.L. Beck, L.S. Katafygiotis, Asymptotic expansions for reliabilities and moments of uncertain dynamic systems, *Journal of Engineering Mechanics, ASCE* 123 (12) (1997) 1219–1229.
[25] T.C. Hsia, *System Identification: Least-Squares Methods*, Lexington Books, D. C. Health and Company, Lexington, MA, Toronto, 1977.